Cancer Letters 449 (2019) 215–225

Contents lists available at ScienceDirect

Cancer Letters

journal homepage: www.elsevier.com/locate/canlet

Original Articles

BRM transcriptionally regulates miR-302a-3p to target SOCS5/STAT3 signaling axis to potentiate pancreatic cancer metastasis

Zhengkui Zhang[a], Jisong Li[a], Huahu Guo[a], Feng Wang[b], Ling Ma[d], Chong Du[a], Yazhou Wang[a], Qi Wang[a], Marko Kornmann[c], Xiaodong Tian[a,**], Yinmo Yang[a,*]

[a] Department of General Surgery, Peking University First Hospital, Beijing, China
[b] Department of Endoscopy Center, Peking University First Hospital, Beijing, China
[c] Clinic of General, Visceral and Transplantation Surgery, University of Ulm, Ulm, Germany
[d] Department of Surgical Oncology, Peking University Ninth School of Clinical Medicine (Beijing Shijitan Hospital, Capital Medical University), Beijing, China

ARTICLE INFO

Keywords:
BRM
miR-302a-3p
SOCS5
STAT3
Pancreatic cancer
Metastasis

ABSTRACT

Brahma (BRM) has recently been documented as a significant predictor of pancreatic cancer (PC) metastasis. This study aimed to further elucidate molecular mechanism by which BRM promotes PC metastasis. We found that silencing BRM reduced PC cell migration and invasion both in vivo and in vitro, accompanied by reduced level of miR-302a-3p. BRM positively regulated the transcription of miR-302a-3p, which acted as a metastasis-promoting miRNA in PC cells. miR-302a-3p directly targeted SOCS5 to boost STAT3 phosphorylation and induce the transcription of STAT3 target genes. Furthermore, miR-302a-3p level was higher in tissue and plasma samples derived from PC patients, and was significantly associated with worse clinical pathological features. In xenograft models, inhibiting miR-302a-3p was synergistically lethal in BRM-silenced PC cells. In conclusion, our results suggest that transcriptional regulation of miR-302a-3p by BRM potentiates PC metastasis by epigenetically suppressing SOCS5 expression and activating STAT3 signaling. These new findings provide potential therapeutic avenues for preventing PC-associated death.

1. Introduction

Pancreatic cancer (PC) is the 7th leading cause of cancer-related deaths worldwide [1]. The 5-year survival rate of PC is very low in the range 5–15% [2]. Metastasis is responsible for most PC-related death as PC is prone to invade adjacent tissues and undergo early metastasis to distal organs [3]. Therefore, patients diagnosed with advanced-stage PC dominate the stage distribution of PC, and only a small subset of patients are eligible for curative surgery [4]. Unfortunately, the majority of postoperative patients experience metastatic relapse, resulting in low 5-year survival rate [5]. Another major reason for the dismal clinical outcomes in PC patients is the resistance to conventional chemoradiotherapy [6]. Elucidation of the mechanisms underlying metastatic potential of PC is urgent to improve therapeutic strategies for PC.

JAK2/STAT3 signaling is constitutively hyperactivated in many solid tumors including PC, and is associated with a worse clinical prognosis [7]. Hyperactivation of JAK2/STAT3 signaling transduces oncogenic signals to promote PC initiation and progression, cancer stem cell maintenance, immunosuppression and therapeutic resistance [8–12]. However, JAK2/STAT3 signaling is negatively modulated by many regulators, including the suppressor of cytokine signaling (SOCS) family, members of the protein inhibitor of activated STAT (PIAS) family, and some phosphatases [13]. SOCS5 is a member of the SOCS family and inhibits the activities of JAK tyrosine kinases [14,15]. A growing amount of evidence indicates that SOCS5 is a tumor suppressor in human cancers by inhibiting both JAK2/STAT3 and EGF receptor pathways. However, the physiological functions of SOCS5 have not been well characterized [16,17]. In addition, some microRNAs (miRNAs) have been shown to target JAK2/STAT3 signaling [18–21]. However, current knowledge on miRNAs as the key regulators of JAK2-STAT3 signaling and their function in PC metastasis is very limited.

Brahma (BRM) is an evolutionarily conserved catalytic ATPase subunit of SWI/SNF chromatin remodeling complexes [22]. Increasing studies have identified BRM as a critical regulator of malignancies [23–27]. Specifically, BRM has been demonstrated to be a significant predictor of PC metastasis and poor prognosis [28]. Our previous study reported that BRM promoted the proliferation and chemoresistance of PC cells by activating JAK2/STAT3 signaling [29]. However, molecular

* Corresponding author. Department of General Surgery, Peking University First Hospital, 8th Xishiku Street, Beijing, China.
** Corresponding author.
E-mail addresses: tianxiaodong@pkufh.cn (X. Tian), yangyinmosci@163.com (Y. Yang).

https://doi.org/10.1016/j.canlet.2019.02.031
Received 4 December 2018; Received in revised form 3 February 2019; Accepted 14 February 2019

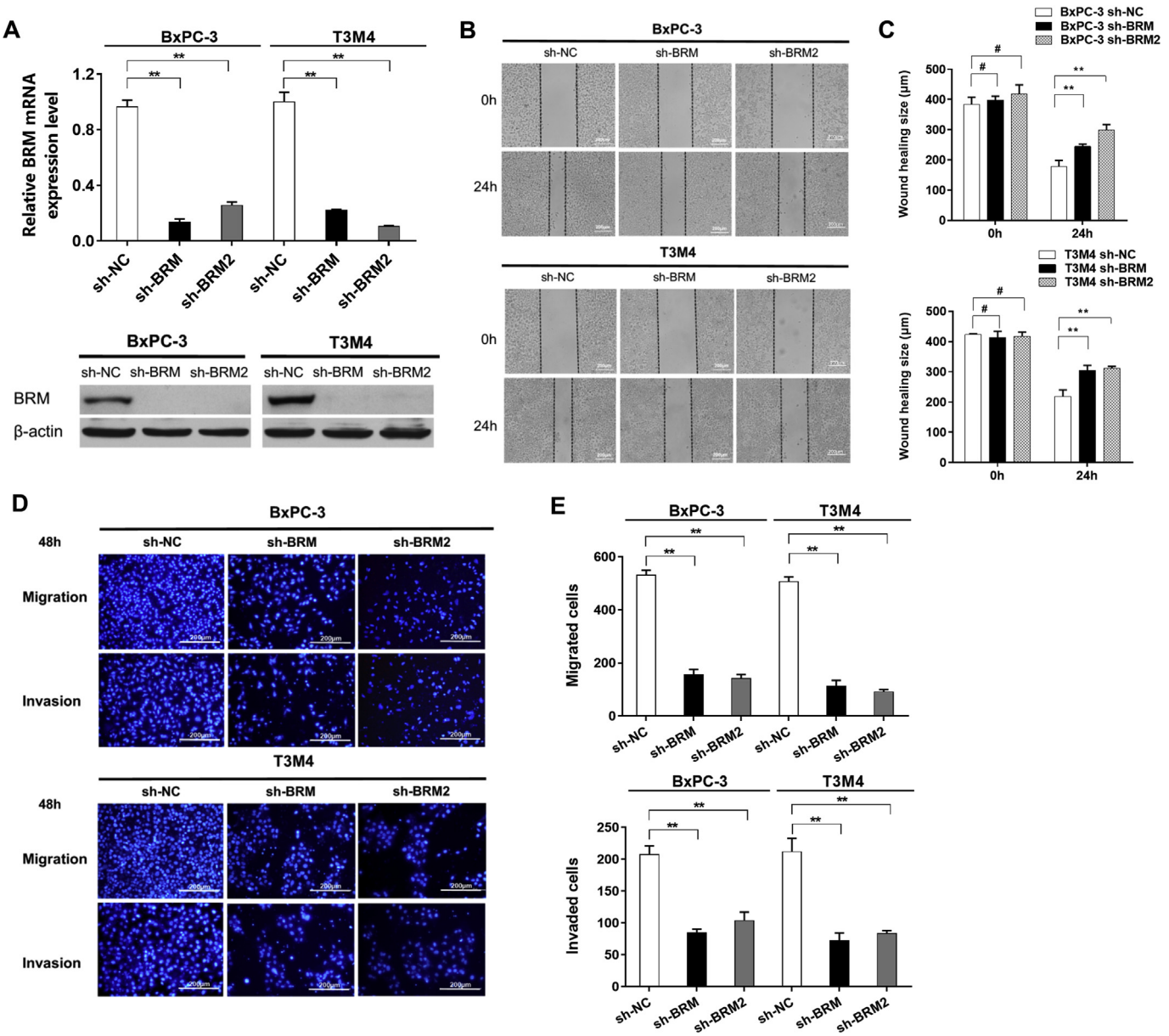

Fig. 1. BRM silencing inhibits PC cell mobility, migration and invasion. (A) The mRNA and protein expression of BRM in BRM knockdown (sh-BRM and sh-BRM2) and negative control (sh-NC) cell lines were detected by qPCR (upper) and Western blot analysis (lower), respectively. GAPDH served as an endogenous control, and β-actin was a loading control. (B) Wound healing assay. Cell monolayers were scratched with a 10 μl pipette tip, and images were then acquired at 0 and 24 h after wound formation. (C) Qualification of the data shown in B (n = 3). (D) Transwell migration and invasion assays using Transwell polycarbonate membranes coated with (invasion) or without (migration) Matrigel. The migrated or invaded cells were imaged at 200 × magnification in five random fields. (E) Qualification of the data shown in D (n = 3). $^{\#}P > 0.05$ and $^{**}P < 0.01$.

mechanisms whereby BRM activates oncogenic signaling to promote PC progression remain unknown. In this study, for the first time we showed that transcriptional regulation of miR-302a-3p by BRM potentiated PC metastasis by targeting SOCS5/STAT3 signaling axis. In addition, we identified circulating miR-302a-3p as a candidate biomarker of PC diagnosis.

2. Materials and methods

2.1. Tissue and plasma specimens

Thirty-five pairs of tumors and adjacent normal tissues were obtained from patients who were pathologically diagnosed with PC at Peking University First Hospital between 2012 and 2017. All specimens were immediately frozen and stored in liquid nitrogen until used. Plasma samples were collected from another 35 PC patients before they underwent surgery or chemotherapy at Peking University First Hospital, and 35 healthy volunteers who served as control group. The volunteers were 20–60 years old and had never suffered from pancreas-related diseases or any tumor. All patients and control volunteers provided written informed consent. This study was approved by the Ethics Committee of Peking University First Hospital.

2.2. Cell culture and transfection

All cell lines used in this study were cultured in recommended medium at 37° in a humidified 5% CO_2 atmosphere and were passaged for fewer than 6 months after resuscitation. All cell lines were recently authenticated by cellular morphology and short tandem repeat analysis using an AmpFLSTR Identifiler PCR Amplification Kit (Invitrogen, CA,

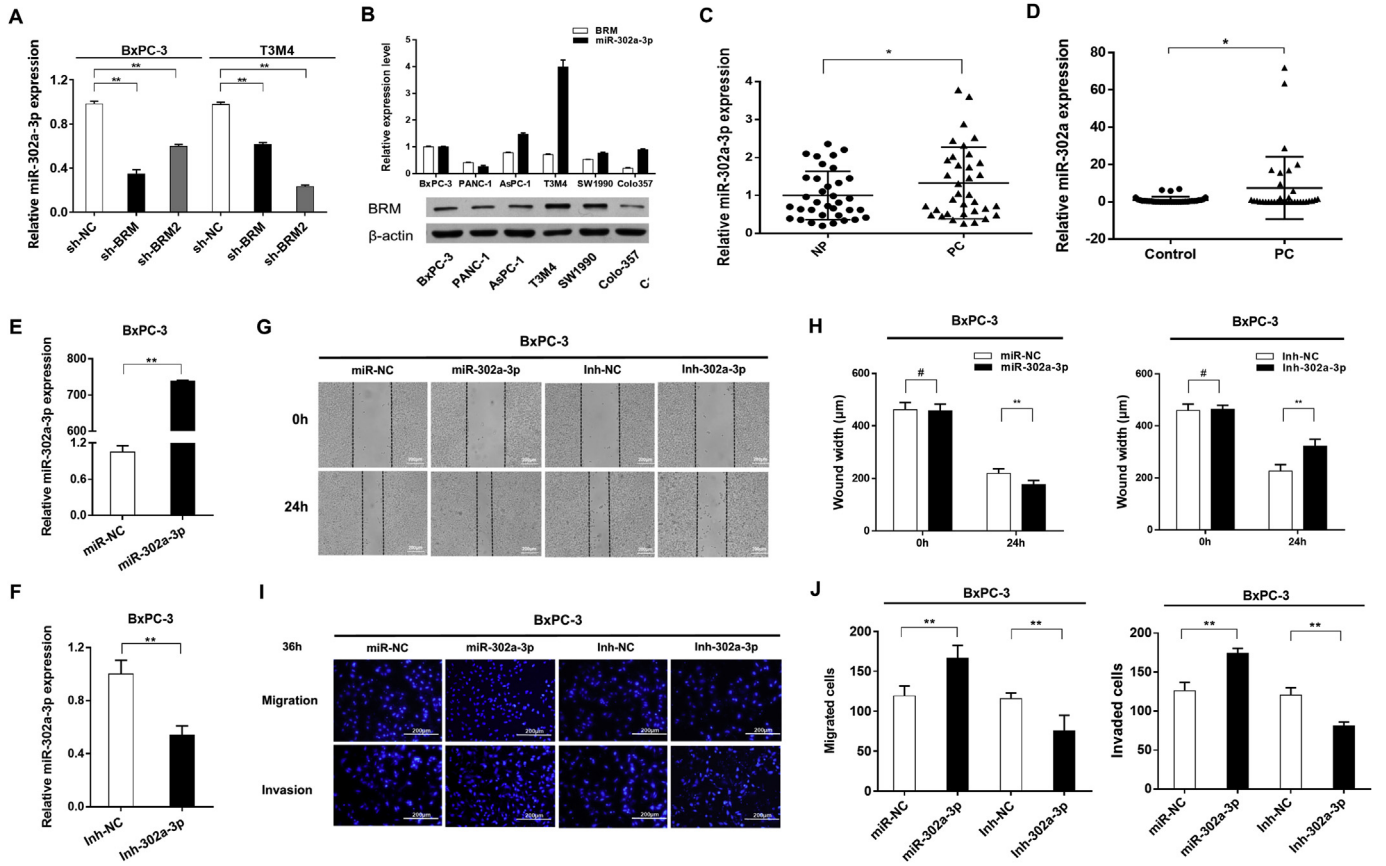

Fig. 2. miR-302a-3p is positively correlated with BRM and acts as a metastasis-promoting miRNA in PC cells. (A) Relative levels of miR-302a-3p in BRM knockdown BxPC-3 and T3M4 cells and control cells measured by qPCR. U6 served as an endogenous control. (B) Relative levels of BRM mRNA and miR-302a-3p in six PC cell lines (upper). BRM protein levels in six PC cell lines detected by Western blot analysis (lower). (C) Relative levels of miR-302a-3p in PC tissues (PC) and paired adjacent non-tumor tissues (NP) measured by qPCR. (D) Circulating miR-302a-3p levels in PC patients and controls detected by qPCR. Cel-miR-39 served as an exogenous control. (E, F) Relative levels of miR-302a-3p in BxPC-3 miR-NC/miR-302a-3p and Inh-NC/Inh-302a-3p cells. (G, H) Wound-healing assay of BxPC-3 miR-NC/miR-302a-3p and Inh-NC/Inh-302a-3p cells. (I, J) Transwell migration and invasion assays of BxPC-3 miR-NC/miR-302a-3p and Inh-NC/Inh-302a-3p cells. $^{\#}P > 0.05$, $^{*}P < 0.05$, $^{**}P < 0.01$.

USA).

A lentiviral vector containing either shRNAs targeting BRM (Gene Bank accession no. NM_003070.4; sh-BRM, GCAGCAGACCGATGAGTA TGT; sh-BRM2, GCTCTTTGCCACCAGATTTAA) or a negative control containing a scrambled sequence (sh-NC, TTCTCCGAACGTGTCACGT TTC) was transfected into 293T cells along with psPAX2 and pMD2.G to produce the lentivirus. Then, stable BRM knockdown BxPC-3 and T3M4 cell lines were established according to the manufacturer's instructions (GenePharma, Shanghai, China).

Mimics and inhibitors of miR-302a-3p and the respective negative control siRNAs were purchased from RiboBio (Guangzhou, China). PC cells were transfected with either 20 nM miR-302a-3p mimic or 60 nM miR-302a-3p inhibitor according to the manufacturer's protocol. Either a mixture of three siRNAs targeting SOCS5 or a negative control was used according to the manufacturer's instructions (GenePharma). The expression vector encoding BRM was designed and constructed by SyngenTech (Beijing, China) using the pLV-pHEF1A-BRM-2A-EGFP-2A-Puro vector. An empty vector was used as the control. Lipofectamine 3000 (Invitrogen) was used as transfection reagent, and transfection efficiency was verified in subsequent experiments.

2.3. Wound healing assay

For wound healing assay, PC cells were seeded in 6-well plates and cultured until complete confluence. Then, a wound was manually introduced into the cell monolayer using a sterile 10 μl pipette tip. The cells were carefully washed three times with PBS (0.01 M, pH 7.4) to remove any floating cells and debris. The cells were then incubated in fresh serum-free RPMI-1640 medium under standard condition. Five random fields were photographed per wound under a microscope (magnification × 100) at two time points (0 h and 24 h), and wound width was measured by *ImageJ* software. Each experiment was performed in triplicate.

2.4. Transwell migration and invasion assay

For migration and invasion assays, PC cells were cultured in serum-free media overnight. Then, 3×10^4 cells in serum-free RPMI-1640 and 6×10^4 cells in serum-free RPMI-1640 were seeded in the upper chambers of 24-well Transwell inserts (Corning, NY, USA) for the migration assays and invasion assays, respectively. The Transwell inserts were precoated with a 1:7 dilution of Matrigel Matrix (Corning) according to the manufacturer's instructions. The lower chambers contained 500 μl of RPMI-1640 supplemented with 10% FBS as the chemoattractant. Next, the cells were cultured under standard condition for 36–48 h. The cells that had migrated or invaded through the polycarbonate membranes were fixed in 4% paraformaldehyde, stained with DAPI, imaged and counted in five random fields under a Fluorescence Inversion Microscope (magnification × 200). Three independent experiments were performed for quantification.

Table 1
Correlations analysis between tissue or plasma miR-302a levels and clinical pathological features in 35 PC patients.

Variables	Tissue				Plasma			
	NO. of cases (n = 35)	miR-302a expression		*P* value	NO. of cases (n = 35)	miR-302a expression		*P* value
		Low (n = 19)	High (n = 16)			Low (n = 27)	High (n = 8)	
Age(years)				0.293				0.700
< 60	13	9 (69.2%)	4 (30.8%)		16	13 (81.2%)	3 (18.8%)	
≥60	22	10 (45.5%)	12 (54.5%)		19	14 (73.7%)	5 (26.3%)	
Gender				0.716				0.691
Male	24	14 (58.3%)	10 (41.7%)		18	13 (72.2%)	5 (27.8%)	
Female	11	5 (45.5%)	6 (54.5%)		17	14 (82.4%)	3 (17.6%)	
Location				1.000				0.166
Head	25	14 (56.0%)	11 (44.0%)		28	20 (71.4%)	8 (28.6%)	
Other	10	5 (50.0%)	5 (50.0%)		7	7 (100%)	0 (0%)	
Tumor size (cm)				0.181				0.032*
< 4	17	7 (41.2%)	10 (58.8%)		22	20 (90.9%)	2 (9.1%)	
≥4	18	12 (66.7%)	6 (33.3%)		13	7 (53.8%)	6 (46.2%)	
Histologic grade				0.700				0.011*
Well/moderate	27	14 (51.9%)	13 (48.1%)		20	19 (95.0%)	1 (5.0%)	
Poor	8	5 (63.5%)	3 (37.5%)		15	8 (53.3%)	7 (46.7%)	
TNM Stage				0.424				0.105
I-II	27	16 (59.3%)	11 (40.7%)		18	16 (88.9%)	2 (11.1%)	
III-IV	8	3 (37.5%)	5 (62.5%)		17	11 (64.7%)	6 (35.3%)	
Primary tumor				1.000				0.154
T1-2	20	11 (55.0%)	9 (45.0%)		8	8 (100%)	0 (0%)	
T3-4	15	8 (53.3%)	7 (46.7%)		27	19 (70.4%)	8 (29.6%)	
Lymphatic invasion				1.000				0.121
Negative	17	9 (52.9%)	8 (47.1%)		16	13 (81.2%)	3 (18.8%)	
Positive	18	10 (55.6%)	8 (44.4%)		19	14 (73.7%)	5 (26.3%)	
Distant metastasis				0.035*				0.648
Negative	31	19 (61.3%)	12 (38.7%)		28	23 (82.1%)	5 (17.9%)	
Positive	4	0 (0%)	4 (100%)		7	4 (57.1%)	3 (42.9%)	
Perineural invasion				0.476				0.387
Negative	12	8 (66.7%)	4 (33.3%)		11	10 (90.9%)	1 (9.1%)	
Positive	23	11 (47.8%)	12 (52.2%)		24	17 (70.8%)	7 (29.2%)	
Vascular invasion				1.000				0.018*
Negative	26	14 (53.8%)	12 (46.2%)		18	17 (94.4%)	1 (5.6%)	
Positive	9	5 (55.6%)	4 (44.4%)		17	10 (58.8%)	7 (41.2%)	

Based on the AJCC Staging System for Pancreatic Adenocarcinoma (8th Edition).
*Statistically significant ($P < 0.05$).

2.5. Real-time quantitative PCR

RNA isolation and real-time quantitative PCR (qPCR) were performed according to protocols previously described [30]. Specifically, U6 and GAPDH were used as the endogenous controls for microRNA and mRNA, respectively. Cel-miR-39 served as the exogenous control for plasma miRNA detection and was not added to plasma samples until TRIZOL reagent (Invitrogen) and chloroform were used. The specific primers for U6, miR-302a-3p and cel-miR-39 were purchased from RiboBio. The other primer sequences were as follows: 5′-GTGCCACAGA AATCCCTCAAA-3' (sense) and 5′-TCTCTTCGTGCAAGTCTTGTTC-3' (antisense) for SOCS5, 5′-AGACCTGGGCAGATTCCAAAC-3' (sense) and 5′-CGGCAAGTCTTCCGAGTAGT-3' (antisense) for MMP9. Each sample was examined in triplicate, and all data were analyzed using the comparative threshold cycle $2^{-\Delta\Delta CT}$ method.

2.6. Western blot analysis and immunohistochemistry

Western blot and immunohistochemistry (IHC) analyses were performed as previously described [29]. The antibody for SOCS5 was purchased from OriGene Technologies (Rockville, MD, USA), and the antibody for MMP9 (ab76003) was obtained from Abcam (Cambridge, MA, USA).

2.7. Chromatin immunoprecipitation assay

Chromatin immunoprecipitation (ChIP) assay was performed according to previously published protocols [31]. In brief, BRM-silenced BxPC-3 cells and control cells were lysed and the lysates were incubated with 2 μg of either normal IgG or BRM antibody. DNA samples were extracted, and qPCR was independently performed three times. The primers were as follows: 5′-GGGACTTCAGCCACTTCTATTT-3' (sense) and 5′-GGAGCACTCATTGTTACCCTAAT-3' (antisense) for miR-302a-3p promoter, 5′-AACGAGCTGGCCTTTCAT-3' (sense) and 5′-GGAGAGAC AGCGCCAAG-3' (antisense) for STAT3 promoter, and 5′-CTCCATTCA GCACTTTCCTCTC-3' (sense) and 5′-AAAGGGAGGAGCCAGTCA-3' (antisense) for SOCS5 promoter. All data were reported as relative values normalized to the level of the input DNA.

2.8. Luciferase assay

Both the 3′UTR fragment of SOCS5, which contains binding sites for miR-302a-3p (WT), and a 3′UTR fragment with a corresponding mutation (Mut) were designed according to the results of bioinformatics prediction. The fragments were inserted into luciferase reporter vector (SyngenTech). BxPC-3 and T3M4 cells were cultured in 96-well plates and transfected with 40 nM of either a miR-302a-3p mimic or a negative control, in combination with 100 ng of either SOCS5 3′UTR WT or Mut reporter using Lipofectamine 3000. After 48 h, the cells were lysed and luciferase activity was measured using luciferase assay kit (Promega, WI, USA) according to the manufacturer's instructions.

2.9. Animal studies

All animal studies were approved and supervised by the Ethics Committee for Animal Use and Care at Peking University First Hospital.

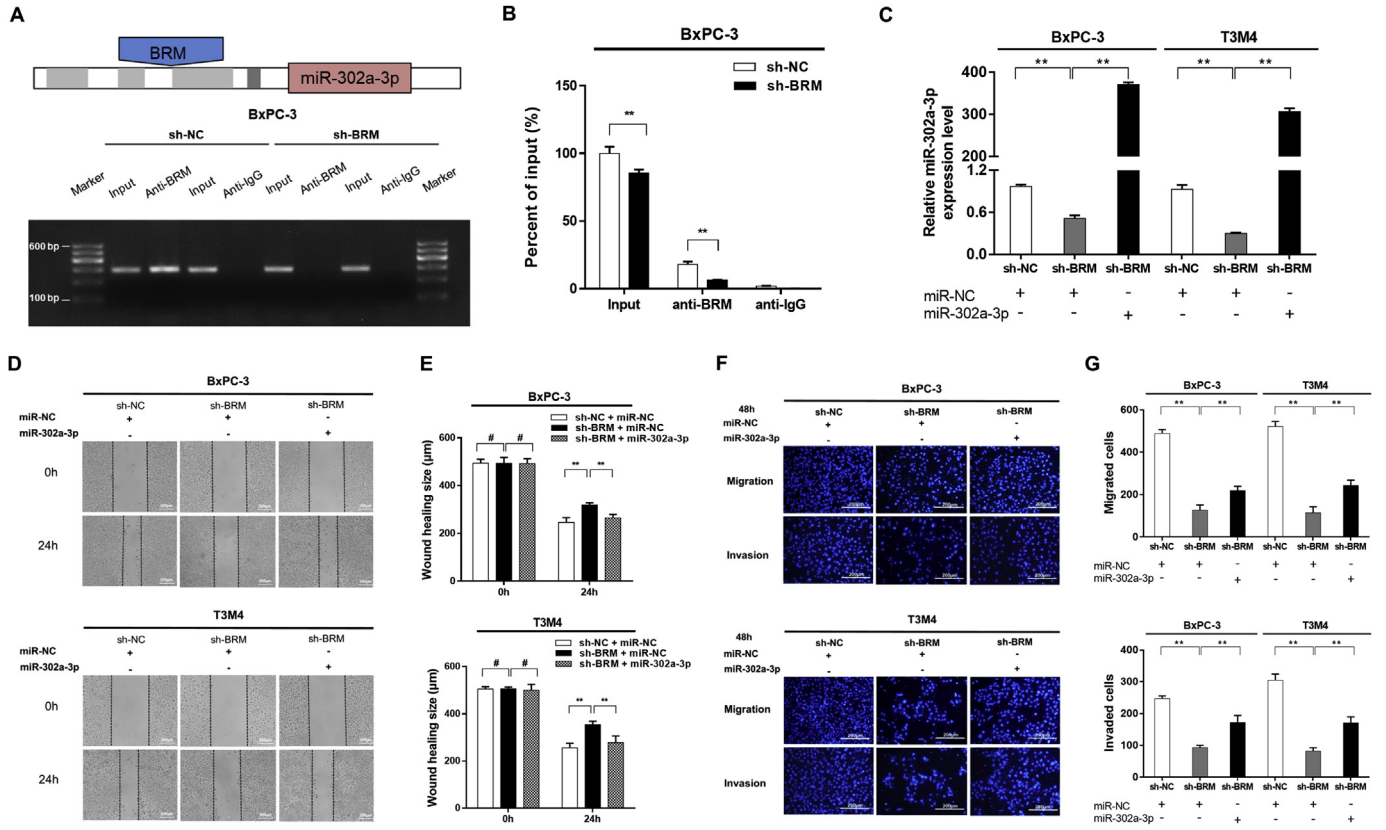

Fig. 3. miR-302a-3p is a target of BRM and restores the mobility, migration and invasion of BRM-silenced cells. (A) Schematic showing the miR-302a-3p promoter with BRM binding sites (upper). ChIP analysis was performed in BxPC-3 sh-NC/sh-BRM cells using anti-IgG and anti-BRM antibodies (lower). (B) DNA fragments were amplified using qPCR with specific oligonucleotides for the miR-302a-3p promoter. (C) miR-302a-3p expression was detected by qPCR in BxPC-3 sh-NC/sh-BRM and T3M4 sh-NC/sh-BRM cells infected with miR-NC or miR-302a-3p. (D, E) Wound-healing assay of BxPC-3 sh-NC/sh-BRM and T3M4 sh-NC/sh-BRM cells infected with miR-NC or miR-302a-3p. (F, G) Transwell migration and invasion assays of BxPC-3 sh-NC/sh-BRM and T3M4 sh-NC/sh-BRM cells infected with miR-NC or miR-302a-3p. $^{\#}P > 0.05$, $^{*}P < 0.05$, $^{**}P < 0.01$.

Nude mice (BALB/c-nu) were purchased and maintained as previously described [32]. For the pulmonary metastasis assay, single cell suspensions containing equal amounts of T3M4 sh-luci-NC or sh-luci-BRM cells (1×10^6 cells in 100 μl of PBS) were injected into the lateral tail vein of five-week-old male nude mice. The metastases in the mice were detected and photographed using an IVIS Spectrum in vivo imaging system (Perkin Elmer, MA, USA) at the study end point. Then, the mice were sacrificed and all lungs were collected for IHC analysis.

To construct xenograft models, equal number of BRM knockdown BxPC-3 cells (1×10^6 cells in 100 μl of PBS) or negative control cells were subcutaneously injected into the bilateral axillary fossae of five-week-old nude mice. When the tumors originating from the BRM-silenced cells reached a volume of 0.1 cm^3, the mice were randomly divided into four groups. Then, 1 nM of miR-302a-3p agomir (mimic), antagomir (inhibitor) or corresponding negative control was injected into the tumors every three days for two weeks. At the study end point, all mice were sacrificed and the tumors were precisely excised and weighed. Tumor growth was monitored throughout the study.

2.10. Statistical analysis

All data are presented as the mean ± standard deviation (SD) and analyzed by SPSS version 19.0 software (SPSS, IL, USA). *P* values were conditionally calculated by paired or unpaired two-tailed Student's *t*-test. ANOVA was performed to compare multiple groups. The relationships between BRM and miR-302a-3p, miR-302a-3p and SOCS5 expression were analyzed using Spearman's rank correlation. Correlations between miR-302a-3p levels and clinical pathological features were analyzed using the Chi-square test. Statistical significance was defined as $P < 0.05$.

3. Results

3.1. BRM silencing inhibits PC cell mobility, migration and invasion

To investigate whether BRM plays a role in PC metastasis, we used two different PC cell lines to establish stable BRM knockdown cell lines (BxPC-3 sh-BRM/sh-BRM2 and T3M4 sh-BRM/sh-BRM2) and negative controls via lentivirus-mediated shRNA transfection. shRNAs targeting BRM effectively decreased BRM mRNA and protein expression in both PC cell lines (Fig. 1A). Wound healing assay showed that knockdown of BRM inhibited the mobility in PC cells (Fig. 1B and C). Transwell migration and invasion assays showed that the number of BRM knockdown BxPC-3 and T3M4 cells that had migrated or invaded through Transwell membranes was lower than that of corresponding control cells (Fig. 1D and E). Taken together, these results demonstrate that BRM silencing inhibited the mobility and migratory and invasive capacity of PC cells.

3.2. miR-302a-3p promotes PC metastasis

miR-302a-3p is an embryonic stem cell-specific miRNA that plays a crucial role in pluripotency maintenance, self-renewal and tumorigenesis [33–36]. We found that miR-302a-3p was expressed at significantly lower levels in BRM-silenced BxPC-3 and T3M4 cells than in control cells (Fig. 2A), suggesting that miR-302a-3p is a potential target of BRM. We then examined the expression levels of miR-302a-3p and BRM in PC lines derived from primary tumors (BxPC-1 or PANC-1), ascites

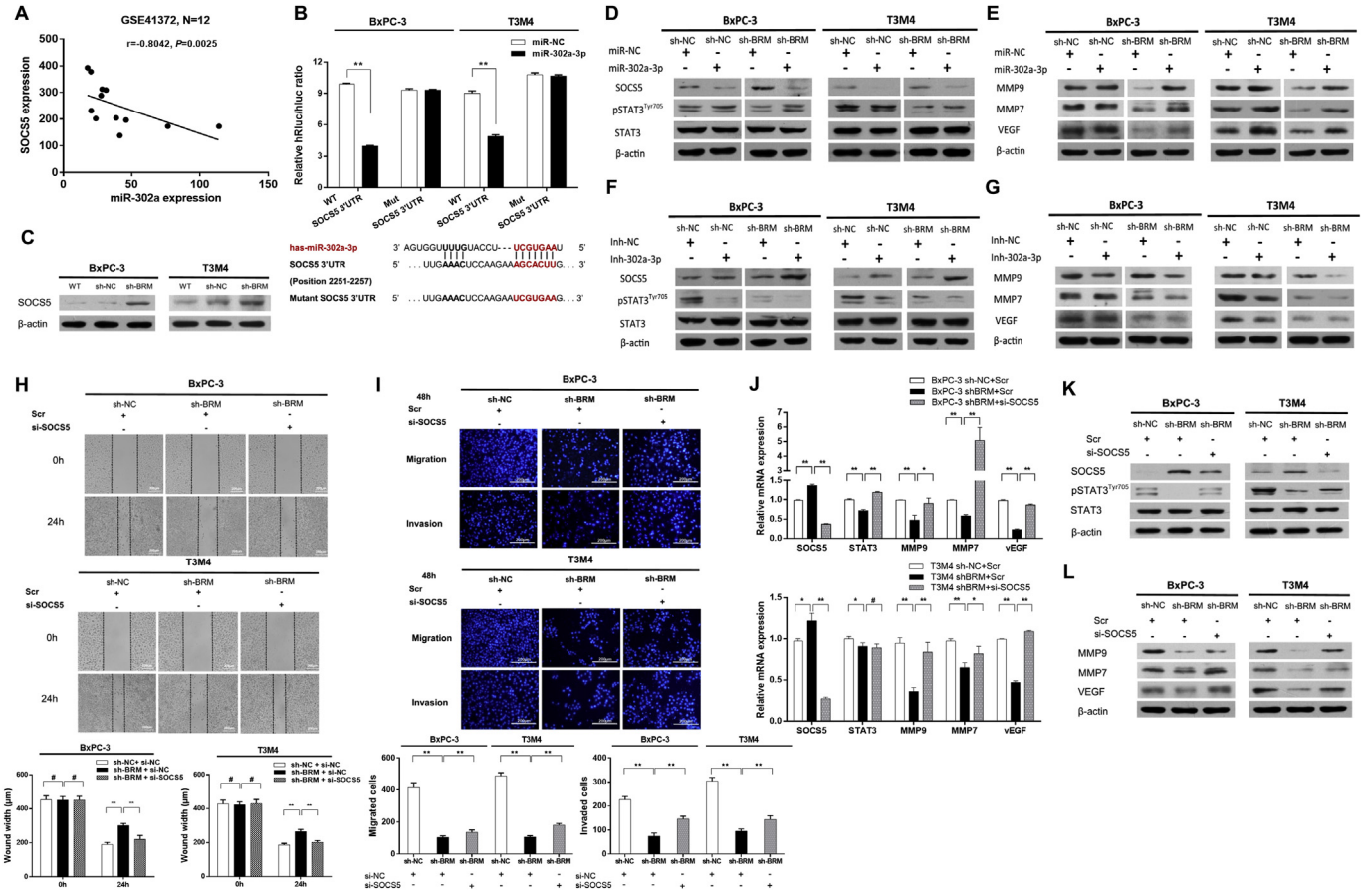

Fig. 4. SOCS5 is a target of miR-302a-3p and BRM regulates SOCS5/STAT3 signaling to mediate PC metastasis. (A) Data mining based on the GEO Database showed a significant negative correlation between miR-302a-3p and SOCS5 levels. (B) 3′UTR fragments of the SOCS5 contain binding sites for miR-302a-3p (WT). Corresponding mutations (Muts) were designed for luciferase assay in BxPC-3 and T3M4 cells. (C) Western blot analysis of SOCS5 protein levels in BxPC-3 sh-NC/sh-BRM, T3M4 sh-NC/sh-BRM cells and wild-type cells (WT). (D–G) Western blot analysis of SOCS5, pSTAT3^{Tyr705}, total STAT3, MMP9, MMP7 and VEGF levels in BRM-silenced BxPC-3, BRM-silenced T3M4 and corresponding negative control cells infected with miR-NC/miR-302a-3p or Inh-NC/Inh-302a-3p. (H, I) Wound-healing assay and Transwell migration and invasion assays of BxPC-3 sh-NC/sh-BRM and T3M4 sh-NC/sh-BRM cells infected with scramble RNA or si-SOCS5 mixture. The mRNA and protein levels of SOCS5, pSTAT3^{Tyr705}, total STAT3, MMP9, MMP7 and VEGF were determined by qPCR (J) and Western blot analysis (K–L). $^{\#}P > 0.05$, $^{*}P < 0.05$, $^{**}P < 0.01$.

(AsPC-1) or metastases (T3M4, SW1990, or Colo-357) [37]. We found that miR-302a-3p and BRM were expressed at different levels in different PC cell lines and the correlation between their expression in PC cell lines tended to be positive (r = 0.6000, $P > 0.05$) (Fig. 2B). Furthermore, miR-302a-3p was expressed at higher levels in PC tissues than in adjacent normal tissues ($P = 0.0218$) (Fig. 2C). Correlation analysis between miR-302a levels in tumor samples and the clinical pathological features of 35 PC patients showed that miR-302a level was significantly correlated with PC metastasis (Table 1, $P = 0.035$).

Plasma miRNAs are potent circulating biomarkers for screening for PC in its early stages and predicting patient survival [38]. We noticed that miR-302a level was remarkably high in plasma samples from seven enrolled patients. To explore the clinical significance of plasma miR-302a-3p level for PC, we expanded the sample size to 35 PC patients and 35 healthy volunteers. While miR-302a-3p was barely detected in plasma samples from healthy volunteers, the level of circulating miR-302a-3p was significantly higher in PC patients ($P = 0.0410$) (Fig. 2D). Furthermore, circulating miR-302a-3p level was significantly correlated with tumor size, histological grade, and vascular invasiveness of PC (Table 1, $P < 0.05$).

To determine the biologic function of miR-302a-3p in PC cells, miR-302a-3p mimic and inhibitor or corresponding negative controls were transfected into BxPC-3 cells (Fig. 2E and F). Wound healing assay showed that overexpressing miR-302a-3p increased the mobility of BxPC-3 cells, while blocking miR-302a-3p inhibited PC cell mobility (Fig. 2G and H). Transwell migration and invasion assays showed that overexpressing miR-302a-3p increased the migration and invasion of BxPC-3 cells, while blocking miR-302a-3p inhibited PC cell migration and invasion (Fig. 2I and J). Taken together, these results suggest that miR-302a-3p expression is positively correlated with BRM expression and PC metastasis, and it functions to promote PC metastasis.

3.3. *miR-302a-3p is a target of BRM and restores the mobility, migration and invasion of BRM-silenced cells*

To explore whether BRM regulates miR-302a-3p expression, we analyzed the promoter region ~2000 bp upstream of the miR-302 stem loop [39,40] and identified a predicted binding site for BRM (Fig. 3A, upper panel). ChIP analysis in BxPC-3 cells showed that BRM bound to the promoter region of miR-302a-3p (Fig. 3A, lower panel) but not to the promoter of SOCS5 or STAT3 (Supplemental Fig. 1). In addition, the amount of immunoprecipitated miR-302a-3p promoter region significantly decreased in BxPC-3 cells with depletion of BRM (Fig. 3B). These data suggest that miR-302a-3p is a transcriptional target of BRM.

To investigate whether miR-302a-3p is an effector of BRM during PC metastasis, we transfected the miR-302a-3p mimic or its negative control into BRM-silenced BxPC-3 and T3M4 cells (Fig. 3C). We found that miR-302a-3p mimic but not miR-NC partially rescued the mobility

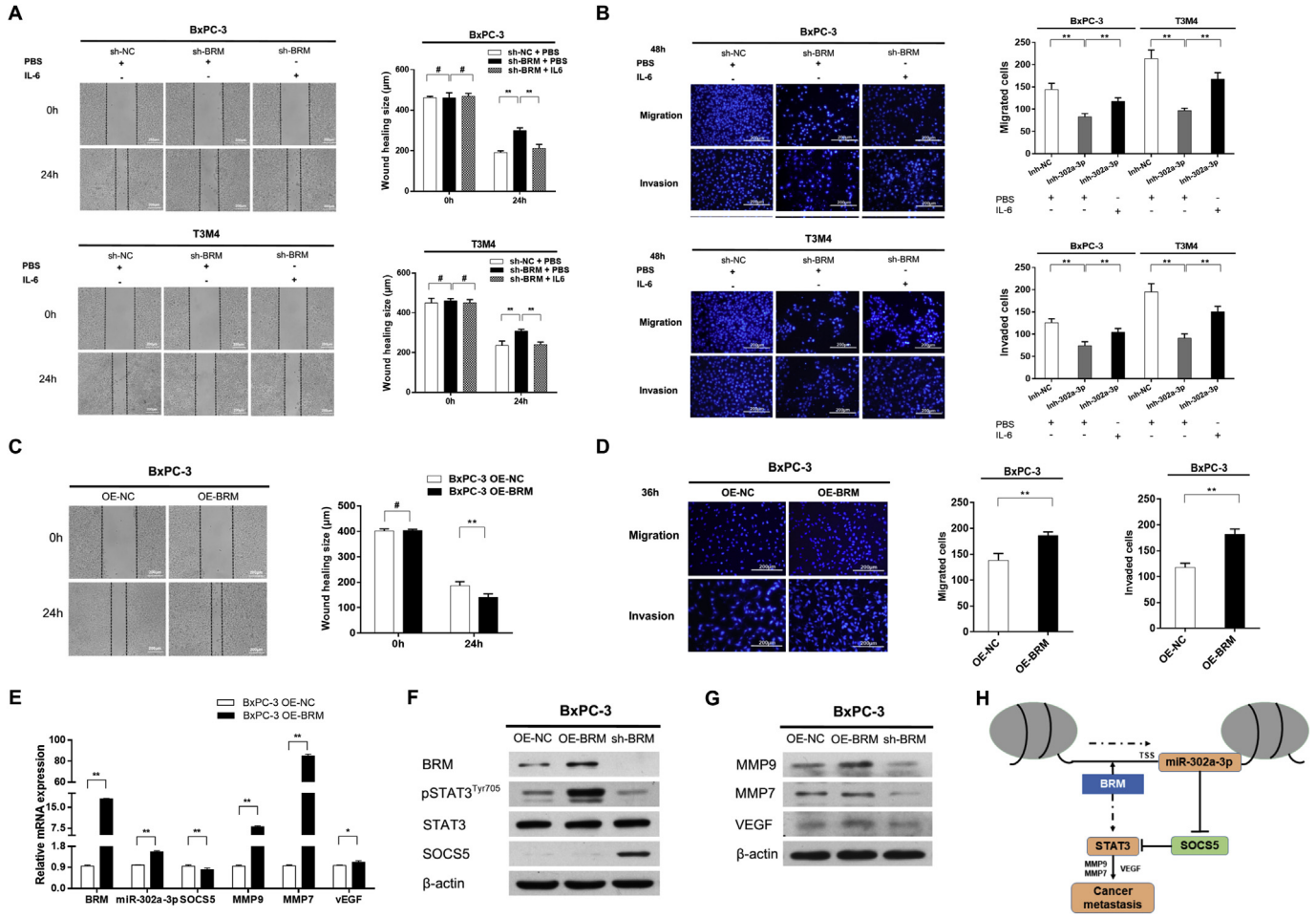

Fig. 5. Exogenous IL-6 restores the mobility, migration and invasion of BRM-silenced PC cells. (A, B) Wound-healing and Transwell migration and invasion assays of BxPC-3 sh-NC/sh-BRM and T3M4 sh-NC/sh-BRM cells treated with or without 100 ng/ml IL-6. (C, D) Wound-healing and Transwell migration and invasion assays of BxPC-3 cells that overexpressed BRM (OE-BRM) and negative control cells (OE-NC). The expression levels of BRM, SOCS5, STAT3, MMP9, MMP7 and VEGF were detected by qPCR (E) and Western blot analysis (F and G). $^{\#}P > 0.05$, $^{*}P < 0.05$, $^{**}P < 0.01$. (H) Schematic diagram showing that BRM transcriptionally regulates miR-302a-3p to potentiate PC metastasis by epigenetically inhibiting SOCS5 expression and activating STAT3 signaling.

of BxPC-3 and T3M4 cells with depletion of BRM (Fig. 3D and E). Transwell migration and invasion assays showed that more cells crossed or invaded the membrane when BRM-silenced PC cells were transfected with miR-302a-3p mimic than when they were transfected with miR-NC (Fig. 3F and G). Collectively, these data demonstrate that miR-302a-3p partially restores the mobility, migration and invasion of BRM-silenced PC cells.

3.4. SOCS5 is a target of miR-302a-3p and BRM regulates SOCS5/STAT3 signaling to promote PC metastasis

BRM activated STAT3 signaling to promote PC cell proliferation and chemoresistance (30). However, it remains unclear how BRM modulate STAT3 signaling axis. A recent study showed that the cooperation of miRNAs inhibited a network of tumor suppressor genes, resulting in tumor progression [41]. A data mining study (http://www.ncbi.nlm.nih.gov/geo/) [42] of the GSE41372 dataset showed that miR-302a-3p was significantly correlated with the expression of SOCS5 ($r = -0.8042$, $P = 0.0025$), which negatively regulated JAK2/STAT3 signaling (Fig. 4A). Bioinformatics analysis confirmed that SOCS5 is a potential target of miR-302a-3p and predicted binding sites for miR-302a-3p in the SOCS5 3′ untranslated region (3′UTR). By luciferase assay we confirmed the direct interaction between miR-302a-3p and SOCS5 (Fig. 4B). In addition, SOCS5 protein was expressed at higher levels in BRM-silenced cells than in control cells, and increased SOCS5 level was correlated with decreased miR-302a-3p level in these cells (Figs. 4C and 2A).

To determine whether SOCS5 is a direct target of miR-302a-3p, we transfected BRM-silenced PC cells with miR-302a-3p mimic, inhibitor or corresponding negative control. We found that overexpressing miR-302a-3p in BRM-silenced cells reduced SOCS5 expression, restored STAT3 phosphorylation and upregulated the expression of MMP9, MMP7 and VEGF (Fig. 4D and E). Conversely, transfecting BRM-silenced cells with miR-302a-3p inhibitor upregulated SOCS5, reduced STAT3 phosphorylation and inhibited the expression of STAT3 target genes (Fig. 4F and G). Furthermore, we used a mixture of three different siRNAs to knockdown SOCS5 in BRM-silenced BxPC-3 and T3M4 cells. The rescue experiment showed that cell mobility restored in BRM-silenced cells transfected with si-SOCS5 mixture but not in the cells transfected with scramble sequence (Fig. 4H). Similarly, cell migration and invasion restored in BRM-silenced cells transfected with si-SOCS5 mixture but not in the cells transfected with scramble sequence (Fig. 4I). In addition, STAT3 phosphorylation recovered and STAT3 target genes were upregulated at both mRNA and protein levels in BRM-silenced cells transfected with si-SOCS5 mixture (Fig. 4J-L). Taken together, these data indicate that SOCS5 is a direct target of miR-302a-3p, and BRM promotes PC metastasis by modulating SOCS5/STAT3 signaling.

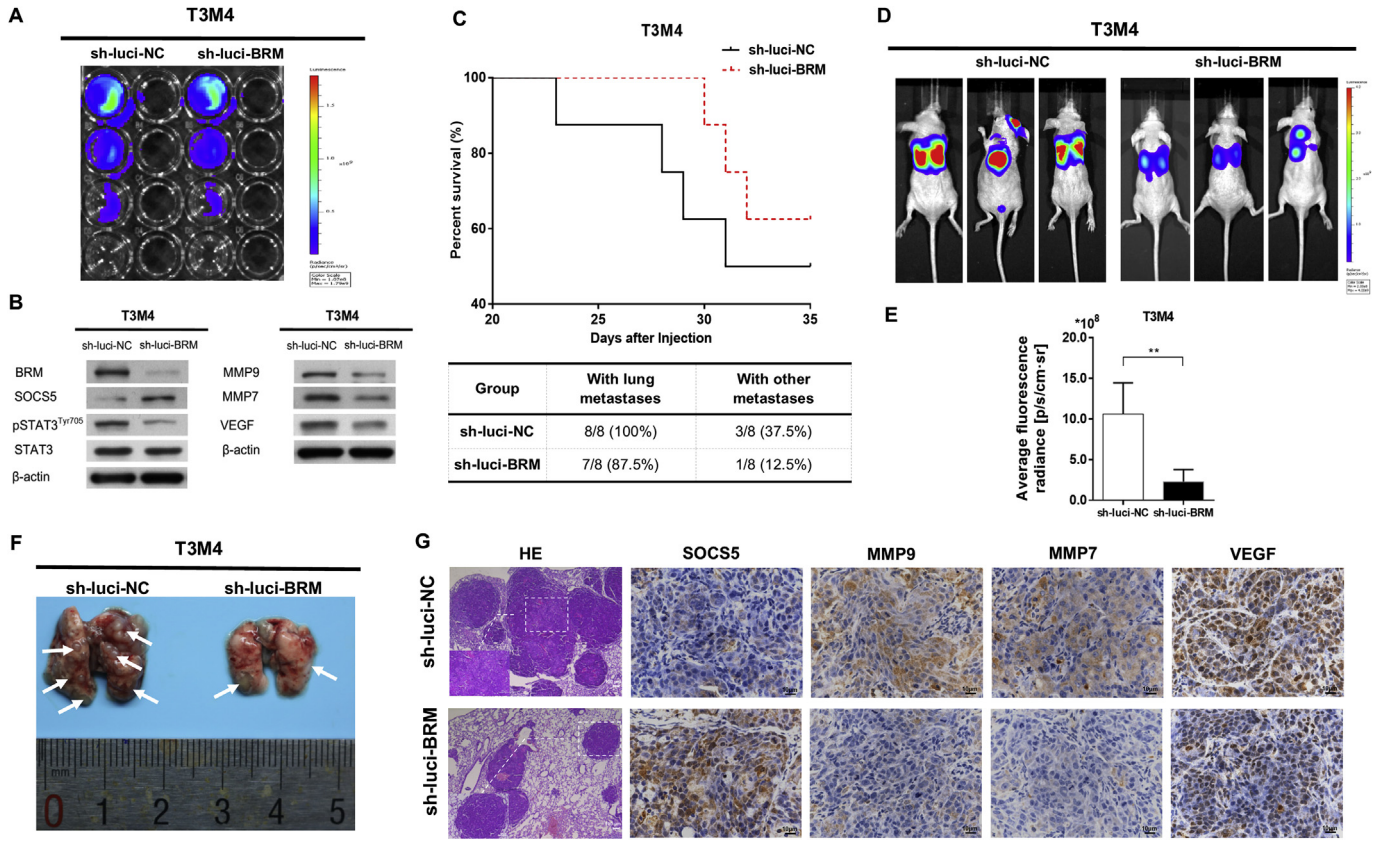

Group	With lung metastases	With other metastases
sh-luci-NC	8/8 (100%)	3/8 (37.5%)
sh-luci-BRM	7/8 (87.5%)	1/8 (12.5%)

Fig. 6. Knockdown of BRM suppresses PC metastasis in vivo. (A) Luciferase expression was detected in T3M4 sh-luci-NC and sh-luci-BRM cells using an IVIS Spectrum system. (B) Western blot analysis of expression levels of BRM and its downstream signaling molecules. (C) The overall rates of survival and metastasis in all nude mice intravenously injected with 1×10^6 PC cells. (D) Representative bioluminescent images of mice at 35 days after injection. (E) Average fluorescence radiance of mice in both groups. $^{**}P < 0.01$. (F) The mice were sacrificed and the lungs were collected. Visible pulmonary metastases were indicated with arrows. (G) Representative images of HE staining of pulmonary metastatic lesions and IHC staining for SOCS5, MMP9, MMP7 and VEGF in pulmonary metastases from mice in both groups.

3.5. Exogenous IL-6 restores the mobility, migration and invasion of BRM-silenced PC cells

Hyperactivation of JAK2/STAT3 signaling plays a vital role in PC metastasis [3,43]. To confirm the involvement of STAT3 signaling in BRM mediated PC metastasis, BxPC-3 and T3M4 cells with depletion of BRM were exposed to IL-6, and their mobility increased (Fig. 5A). Similarly, the migration and invasion of BxPC-3 and T3M4 cells with depletion of BRM increased after exposure to IL-6 (Fig. 5B). Furthermore, we found that overexpression of BRM in BxPC-3 cells enhanced cell mobility, migration and invasion (Fig. 5C and D). These phenotypic changes were correlated to decreased SOCS5 expression, increased miR-302a-3p level, increased STAT3 phosphorylation and the upregulation of STAT3 target genes (Fig. 5E–G). In summary, these findings suggest that BRM transcriptionally regulates miR-302a-3p to potentiate PC metastasis by targeting SOCS5/STAT3 signaling axis (Fig. 5H).

3.6. Knockdown of BRM suppresses PC metastasis in vivo

To verify the effects of BRM on PC metastasis in vivo, T3M4 cells expressing a luciferase reporter were used to construct BRM-silenced (sh-luci-BRM) and control (sh-luci-NC) cells. Luciferase and BRM expression was confirmed in both cell lines by IVIS Spectrum imaging and Western blot analysis (Fig. 6A and B). Next, single cell suspensions containing equal amounts of T3M4 sh-luci-NC (test group) or sh-luci-BRM (control group) cells were injected into the lateral tail veins of nude mice.

At 35 days after injection, the mice in test group had a better prognosis and survival than in control group (Fig. 6C, upper panel). Furthermore, we compared the average fluorescence radiance of both groups on an IVIS Spectrum in vivo imaging system, and the capacity to form pulmonary metastases was lower in T3M4 sh-luci-BRM cells than in control cells (Fig. 6D and E). Bioluminescent images indicated metastases in the lungs of most of test group mice (7/8) and all of the mice in control group. While 3/8 of the mice in control group had additional metastases (1 in the supramaxillar and 2 in the lumbar vertebrae), only 1/8 of test group mice exhibited metastasis in the thoracic vertebrae (Fig. 6C, lower panel). Compared to control group, mice in test group exhibited fewer visible pulmonary metastases (Fig. 6F). In addition, IHC staining showed higher SOCS5 level in pulmonary metastases obtained from test group than from control group, while STAT3 targets MMP9, MMP7 and VEGF were significantly downregulated by BRM silencing (Fig. 6G). Collectively, these data indicate that BRM promotes PC metastasis in vivo by targeting SOCS5/STAT3 signaling.

3.7. Inhibiting miR-302a-3p is a potential epigenetic approach to PC therapy

The above results suggest that interfering with miR-302a-3p may represent a targeted approach to PC therapy. We therefore hypothesized that simultaneously suppressing both BRM and miR-302a-3p might represent a synergistically beneficial PC treatment. BxPC-3 cells with depletion of BRM or negative control cells were subcutaneously injected into the bilateral axillary fossae of twenty male nude mice (Fig. 7A). When the tumors that originated from the BRM-silenced cells reached a certain size (0.1 cm^3) on the 14th day after injection, the mice

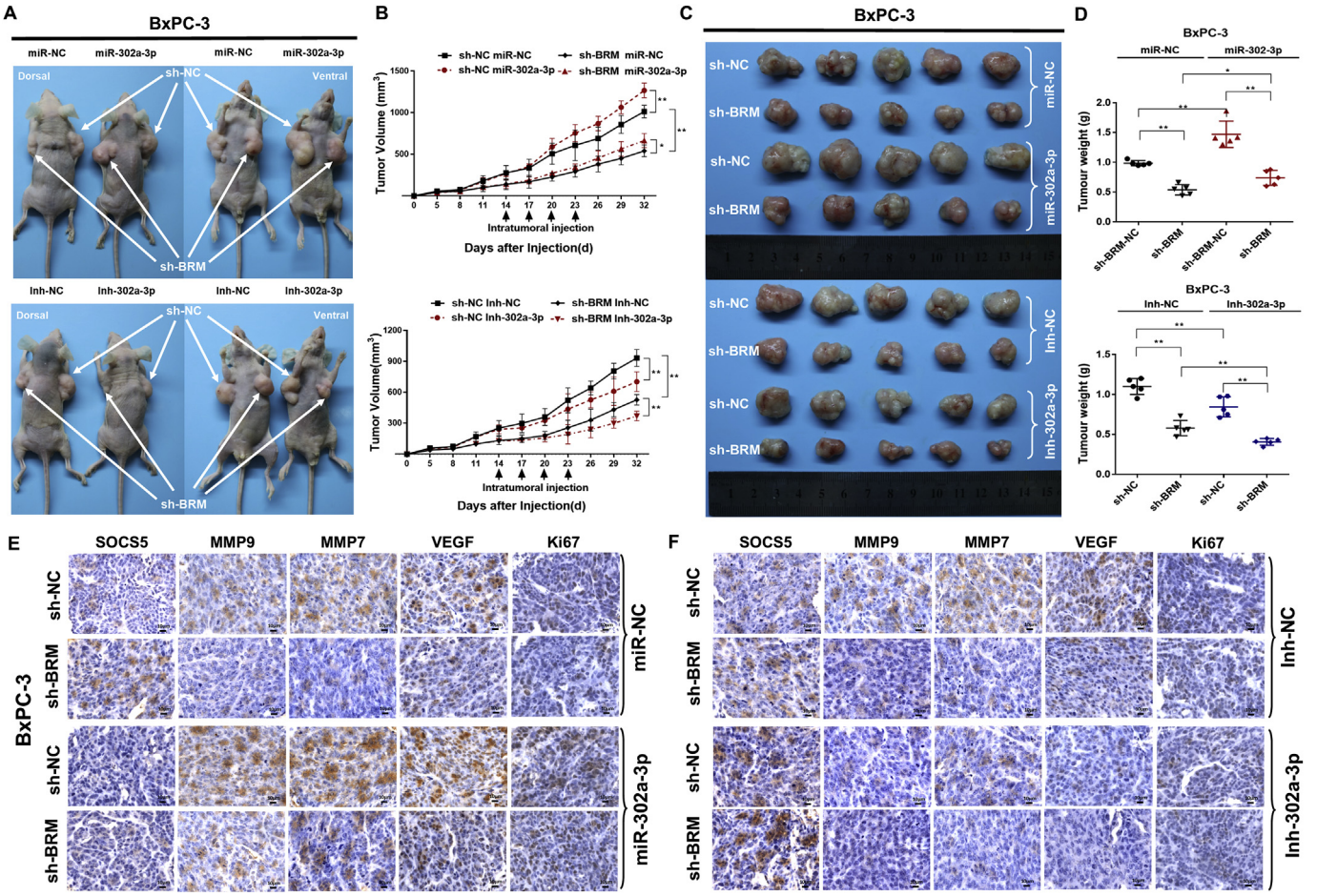

Fig. 7. Inhibiting miR-302a-3p is a potential epigenetic approach to PC therapy. (A) BRM knockdown BxPC-3 or negative control cells were injected into twenty male nude mice, which were divided into four groups on the 14th day after injection. Then, 1 nM of miR-302a-3p agomir, antagomir or corresponding negative control was intratumorally injected into the tumors every three days for two weeks. (B) Tumor volume was measured in all groups every three days beginning on the fifth day after injection until the study end point to determine growth curve. (C) Tumors derived from all groups are presented. (D) Tumor mass was measured in all groups and compared ($^{*}P < 0.05$, $^{**}P < 0.01$, paired *t*-test). (E) and (F) Representative images of IHC staining for SOCS5, MMP9, MMP7, VEGF and Ki67 in tumors obtained from mice in both groups. $^{*}P < 0.05$, $^{**}P < 0.01$.

were randomly divided into four groups (n = 5). Then, 1 nM of a miR-302a-3p agomir (mimic), antagomir (inhibitor) or corresponding negative control was injected into the tumors every three days for two weeks. When the tumors from control cells reached a certain size (1.0 cm^3), all of the mice were sacrificed, and the tumors were carefully excised and weighed.

We found that tumors derived from sh-BRM cells grew slower and had smaller volume than the tumors originating from control cells, and tumor growth was accelerated by the intratumoral injection of miR-302a-3p agomir but was decelerated by miR-302a-3p antagomir (Fig. 7B). Intratumoral injection of miR-302a-3p antagomir further reduced tumor burden (Fig. 7C and D, lower panel), while miR-302a-3p agomir promoted tumor growth by counteracting the effects of BRM silencing (Fig. 7C and D, upper panel). In addition, IHC staining indicated that miR-302a-3p agomir decreased SOCS5 expression but increased the expression of STAT3 targets and Ki67, thereby compensating for the deficient STAT3 signaling in BRM-silenced cells (Fig. 7E). However, miR-302a-3p antagomir increased SOCS5 expression and decreased STAT3 signaling, thereby inhibiting the expression of STAT3 target genes and Ki67 synergistically with BRM silencing (Fig. 7F). Collectively, these data indicate that inhibiting miR-302a-3p is synthetic lethal when combined with BRM silencing in PC cells.

4. Discussion

In this study, we report that knockdown of BRM reduced PC cell migration and invasion both in vivo and in vitro, and these effects were associated with the downregulation of miR-302a-3p. Moreover, BRM positively regulated the transcription of miR-302a-3p, which was identified as a metastasis-promoting miRNA in PC cells. Mechanistically, we reveal that miR-302a-3p directly targets SOCS5, a negative regulator of STAT3 signaling, to boost STAT3 phosphorylation and consequently induce the transcription of STAT3 target genes. Furthermore, miR-302a-3p level was higher in tissue and plasma samples from PC patients and was significantly associated with worse clinical pathological features. In vivo experiments demonstrated that inhibiting miR-302a-3p was synergistically lethal with BRM silencing in PC cells, suggesting a potential epigenetic approach to PC therapy.

BRM is known to alter the accessibility of DNA regions for transcription, and is involved in development, differentiation, metabolism, proliferation, apoptosis, cell adhesion, DNA repair, and signal transduction [44]. A growing amount of evidence suggests that BRM is a tumor suppressor because it is frequently inactivated in a variety of tumor types [23,24]. However, other studies showed that aberrant expression of BRM is essential for cancer initiation and development [25–27]. Therefore, in this study we used two different PC cell lines (BxPC-3 and T3M4) to establish stable BRM knockdown cell lines via lentivirus-mediated shRNA transfection. We then confirmed that

silencing BRM reduced PC cell migration and invasion both in vivo and in vitro.

To elucidate the mechanisms by which BRM promotes PC metastasis, we focused on so-called “metastamirs”, which contribute to post-transcriptional regulation of cellular metastatic competence [45–47]. MiR-302a-3p plays crucial role in pluripotency maintenance, self-renewal and tumorigenesis [33–36]. In this study, we showed that miR-302a-3p is expressed at different levels among PC cell lines and is up-regulated in PC tissues. The expression of miR-302a-3p was associated with poor M-stage in clinical PC samples. Moreover, circulating miR-302a-3p level was higher in plasma samples from PC patients and was significantly correlated with tumor size, histologic grade, and vascular invasion. Next, we confirmed that miR-302a-3p acted as a metastasis-promoting miRNA in PC cells. ChIP assay showed that miR-302a-3p transcription is directly regulated by BRM. It is important to note that miR-302a-3p is only one downstream target of BRM. Other targets of BRM could also contribute to the regulation of PC cell mobility, migration and invasion. Thus overexpression of miR-302a-3p only partially restored the mobility, migration and invasion of BRM-silenced PC cells.

Next we analyzed the GSE28735 dataset [41], and found that miR-302a-3p is aberrantly expressed in PC specimens and cell lines, and its expression is significantly correlated with SOCS5, a negatively regulator of JAK2/STAT3 signaling. Bioinformatics analysis and luciferase assay further verified that miR-302a-3p binds directly to the 3′UTR of SOCS5. We found that SOCS5 protein expression was higher in BRM-silenced cells than in control cells, in agreement with the decline in miR-302a-3p level in these cells. Notably, rescuing the expression of miR-302a-3p in BRM-silenced cells reduced SOCS5 protein level, restored STAT3 phosphorylation and upregulated the expression of MMP9, MMP7 and VEGF. Conversely, transfection of miR-302a-3p inhibitor into BRM-silenced cells increased SOCS5 level, reduced STAT3 phosphorylation and inhibited the expression of STAT3 target genes. Likewise, silencing SOCS5 in BRM knockdown cells significantly reversed the phenotypic changes and re-activated JAK2/STAT3 signaling. Collectively, these results indicate that the effect of BRM on PC metastasis is mediated by miR-302a-3p, which directly targets SOCS5. These data suggest that BRM integrates epigenetic regulatory network and oncogenic signal transduction to potentiate PC metastasis.

Based on the results of in vitro experiments, we hypothesized that simultaneously suppressing both BRM and miR-302a-3p might represent a synergistically beneficial PC treatment. We then constructed xenograft models using BRM-silenced PC cells and administrated miR-302a-3p mimic or inhibitor. While tumors derived from BRM-silenced cells grew slower than those derived from control cells, intratumoral injection of miR-302a-3p agomir accelerated the growth of tumors derived from BRM-silenced cells. In contrast, intratumoral injection of miR-302a-3p antagomir further inhibited the growth of tumors derived from BRM-silenced cells. IHC analysis showed that SOCS5 protein and STAT3 target gene expression levels were correlated with the modulation of miR-302a-3p level in the tumors. These data provide strong evidence that inhibiting miR-302a-3p synergizes with BRM knockdown to inhibit PC.

In conclusion, transcriptional activation of miR-302a-3p by BRM potentiates PC metastasis by targeting SOCS5/STAT3 signaling axis in both cell culture and in vivo models. In addition, circulating miR-302a-3p is a potential biomarker for PC diagnosis, and inhibiting miR-302a-3p is synergistically lethal with BRM silencing in PC cells due to augmented inhibition of JAK2/STAT3 signaling. These new findings would facilitate the development of novel early detection and therapeutic strategies for PC.

Competing interests

The authors have declared that no competing interest exists.

Acknowledgements

This work was supported in part by grants 81372605 (to Y. Yang), 81572339 (to X. Tian), 81672353 and 81871954 (to Y. Yang) from the National Natural Science Foundation of China and grant SS2015AA020405 from the National High Technology Research and Development Program of China (to Y. Yang). We sincerely appreciate the technical support by Prof. Zebin Mao of the Department of Biochemistry and Molecular Biology in Peking University Health Science Center. We thank Jinhui Yu from the Department of Epidemiology and Biostatistics in Peking University Health Science Center for providing support with the statistical analyses. The authors also thank Jing Zhu from the Department of General Surgery, Peking University First Hospital, for her clinical and technical advice regarding the management of patient specimens.

Appendix A. Supplementary data

Supplementary data to this article can be found online at https://doi.org/10.1016/j.canlet.2019.02.031.

References

[1] L.A. Torre, F. Bray, R.L. Siegel, J. Ferlay, J. Lortet-Tieulent, A. Jemal, Global cancer statistics, 2012, CA Cancer J Clin 65 (2015) 87–108.
[2] C. Allemani, T. Matsuda, V. Di Carlo, R. Harewood, M. Matz, M. Niksic, A. Bonaventure, M. Valkov, C.J. Johnson, J. Esteve, O.J. Ogunbiyi, E.S.G. Azevedo, W.Q. Chen, S. Eser, G. Engholm, C.A. Stiller, A. Monnereau, R.R. Woods, O. Visser, G.H. Lim, J. Aitken, H.K. Weir, M.P. Coleman, Global surveillance of trends in cancer survival 2000-14 (CONCORD-3): analysis of individual records for 37 513 025 patients diagnosed with one of 18 cancers from 322 population-based registries in 71 countries, Lancet (London, England) 391 (2018) 1023–1075.
[3] E. Giovannetti, C.L. van der Borden, A.E. Frampton, A. Ali, O. Firuzi, G.J. Peters, Never let it go: stopping key mechanisms underlying metastasis to fight pancreatic cancer, Semin. Canc. Biol. 44 (2017) 43–59.
[4] T. Kamisawa, L.D. Wood, T. Itoi, K. Takaori, Pancreatic cancer, Lancet (London, England) 388 (2016) 73–85.
[5] I. Garrido-Laguna, M. Hidalgo, Pancreatic cancer: from state-of-the-art treatments to promising novel therapies, Nature reviews, Clin. Oncol. 12 (2015) 319–334.
[6] A.H. Ko, Progress in the treatment of metastatic pancreatic cancer and the search for next opportunities, J. Clin. Oncol.: Off. J. Am. Soc. Clin. Oncol. 33 (2015) 1779–1786.
[7] H. Yu, H. Lee, A. Herrmann, R. Buettner, R. Jove, Revisiting STAT3 signalling in cancer: new and unexpected biological functions, Nat. Rev. Canc. 14 (2014) 736–746.
[8] R.B. Corcoran, G. Contino, V. Deshpande, A. Tzatsos, C. Conrad, C.H. Benes, D.E. Levy, J. Settleman, J.A. Engelman, N. Bardeesy, STAT3 plays a critical role in KRAS-induced pancreatic tumorigenesis, Cancer Res. 71 (2011) 5020–5029.
[9] M. Lesina, M.U. Kurkowski, K. Ludes, S. Rose-John, M. Treiber, G. Kloppel, A. Yoshimura, W. Reindl, B. Sipos, S. Akira, R.M. Schmid, H. Algul, Stat3/Socs3 activation by IL-6 transsignaling promotes progression of pancreatic intraepithelial neoplasia and development of pancreatic cancer, Cancer Cell 19 (2011) 456–469.
[10] N. Tyagi, S. Marimuthu, A. Bhardwaj, S.K. Deshmukh, S.K. Srivastava, A.P. Singh, S. McClellan, J.E. Carter, S. Singh, p-21 activated kinase 4 (PAK4) maintains stem cell-like phenotypes in pancreatic cancer cells through activation of STAT3 signaling, Cancer Lett. 370 (2016) 260–267.
[11] C. Lu, A. Talukder, N.M. Savage, N. Singh, K. Liu, JAK-STAT-mediated chronic inflammation impairs cytotoxic T lymphocyte activation to decrease anti-PD-1 immunotherapy efficacy in pancreatic cancer, OncoImmunology 6 (2017) e1291106.
[12] N.S. Nagathihalli, J.A. Castellanos, C. Shi, Y. Beesetty, M.L. Reyzer, R. Caprioli, X. Chen, A.J. Walsh, M.C. Skala, H.L. Moses, N.B. Merchant, Signal transducer and activator of transcription 3, mediated remodeling of the tumor microenvironment results in enhanced tumor drug delivery in a mouse model of pancreatic cancer, Gastroenterology 149 (2015) 1932–1943 e1939.
[13] D.E. Johnson, R.A. O'Keefe, J.R. Grandis, Targeting the IL-6/JAK/STAT3 signalling axis in cancer, Nat. Rev. Clin. Oncol. 15 (2018) 234–248.
[14] E.M. Linossi, S.E. Nicholson, Kinase inhibition, competitive binding and proteasomal degradation: resolving the molecular function of the suppressor of cytokine signaling (SOCS) proteins, Immunol. Rev. 266 (2015) 123–133.
[15] I.R. Chandrashekaran, B. Mohanty, E.M. Linossi, L.F. Dagley, E.W. Leung, J.M. Murphy, J.J. Babon, S.E. Nicholson, R.S. Norton, Structure and functional characterization of the conserved JAK interaction region in the intrinsically disordered N-terminus of SOCS5, Biochemistry 54 (2015) 4672–4682.
[16] M. Jiang, W.W. Zhang, P. Liu, W. Yu, T. Liu, J. Yu, Dysregulation of SOCS-mediated negative feedback of cytokine signaling in carcinogenesis and its significance in cancer treatment, Front. Immunol. 8 (2017) 70.
[17] S. Chikuma, M. Kanamori, S. Mise-Omata, A. Yoshimura, Suppressors of cytokine signaling: potential immune checkpoint molecules for cancer immunotherapy,

Cancer Sci. 108 (2017) 574–580.
[18] J. Jiang, Z. Li, C. Yu, M. Chen, S. Tian, C. Sun, MiR-1181 inhibits stem cell-like phenotypes and suppresses SOX2 and STAT3 in human pancreatic cancer, Cancer Lett. 356 (2015) 962–970.
[19] K. Patel, A. Kollory, A. Takashima, S. Sarkar, D.V. Faller, S.K. Ghosh, MicroRNA let-7 downregulates STAT3 phosphorylation in pancreatic cancer cells by increasing SOCS3 expression, Cancer Lett. 347 (2014) 54–64.
[20] G. Zhuang, X. Wu, Z. Jiang, I. Kasman, J. Yao, Y. Guan, J. Oeh, Z. Modrusan, C. Bais, D. Sampath, N. Ferrara, Tumour-secreted miR-9 promotes endothelial cell migration and angiogenesis by activating the JAK-STAT pathway, EMBO J. 31 (2012) 3513–3523.
[21] C. Huang, H. Li, W. Wu, T. Jiang, Z. Qiu, Regulation of miR-155 affects pancreatic cancer cell invasiveness and migration by modulating the STAT3 signaling pathway through SOCS1, Oncol. Rep. 30 (2013) 1223–1230.
[22] J. Masliah-Planchon, I. Bieche, J.M. Guinebretiere, F. Bourdeaut, O. Delattre, SWI/SNF chromatin remodeling and human malignancies, Ann. Rev. Pathol. 10 (2015) 145–171.
[23] H. Itamochi, T. Oishi, N. Oumi, S. Takeuchi, K. Yoshihara, M. Mikami, N. Yaegashi, Y. Terao, K. Takehara, K. Ushijima, H. Watari, D. Aoki, T. Kimura, T. Nakamura, Y. Yokoyama, J. Kigawa, T. Sugiyama, Whole-genome sequencing revealed novel prognostic biomarkers and promising targets for therapy of ovarian clear cell carcinoma, Br. J. Canc. 117 (2017) 717–724.
[24] C. Kadoch, D.C. Hargreaves, C. Hodges, L. Elias, L. Ho, J. Ranish, G.R. Crabtree, Proteomic and bioinformatic analysis of mammalian SWI/SNF complexes identifies extensive roles in human malignancy, Nat. Genet. 45 (2013) 592–601.
[25] A. Sun, O. Tawfik, B. Gayed, J.B. Thrasher, S. Hoestje, C. Li, B. Li, Aberrant expression of SWI/SNF catalytic subunits BRG1/BRM is associated with tumor development and increased invasiveness in prostate cancers, Prostate 67 (2007) 203–213.
[26] B. Keenen, H. Qi, S.V. Saladi, M. Yeung, I.L. de la Serna, Heterogeneous SWI/SNF chromatin remodeling complexes promote expression of microphthalmia-associated transcription factor target genes in melanoma, Oncogene 29 (2010) 81–92.
[27] Q. Wu, P. Madany, J. Akech, J.R. Dobson, S. Douthwright, G. Browne, J.L. Colby, G.E. Winter, J.E. Bradner, J. Pratap, G. Sluder, R. Bhargava, S.I. Chiosea, A.J. van Wijnen, J.L. Stein, G.S. Stein, J.B. Lian, J.A. Nickerson, A.N. Imbalzano, The SWI/SNF ATPases are required for triple negative breast cancer cell proliferation, J. Cell. Physiol. 230 (2015) 2683–2694.
[28] M. Numata, S. Morinaga, T. Watanabe, H. Tamagawa, N. Yamamoto, M. Shiozawa, Y. Nakamura, Y. Kameda, S. Okawa, Y. Rino, M. Akaike, M. Masuda, Y. Miyagi, The clinical significance of SWI/SNF complex in pancreatic cancer, Int. J. Oncol. 42 (2013) 403–410.
[29] Z. Zhang, F. Wang, C. Du, H. Guo, L. Ma, X. Liu, M. Kornmann, X. Tian, Y. Yang, BRM/SMARCA2 promotes the proliferation and chemoresistance of pancreatic cancer cells by targeting JAK2/STAT3 signaling, Cancer Lett. 402 (2017) 213–224.
[30] L. Ma, X. Tian, H. Guo, Z. Zhang, C. Du, F. Wang, X. Xie, H. Gao, Y. Zhuang, M. Kornmann, H. Gao, Y. Yang, Long noncoding RNA H19 derived miR-675 regulates cell proliferation by down-regulating E2F-1 in human pancreatic ductal adenocarcinoma, J. Canc. 9 (2018) 389–399.
[31] J. Yang, K. Liu, J. Yang, B. Jin, H. Chen, X. Zhan, Z. Li, L. Wang, X. Shen, M. Li, W. Yu, Z. Mao, PIM1 induces cellular senescence through phosphorylation of UHRF1 at Ser311, Oncogene 36 (2017) 4828–4842.
[32] F. Wang, L. Ma, Z. Zhang, X. Liu, H. Gao, Y. Zhuang, P. Yang, M. Kornmann, X. Tian, Y. Yang, Hedgehog signaling regulates epithelial-mesenchymal transition in pancreatic cancer stem-like cells, J. Canc. 7 (2016) 408–417.
[33] Z. Zhang, Y. Hong, D. Xiang, P. Zhu, E. Wu, W. Li, J. Mosenson, W.S. Wu, MicroRNA-302/367 cluster governs hESC self-renewal by dually regulating cell cycle and apoptosis pathways, Stem Cell Reports 4 (2015) 645–657.
[34] L.Y. Bourguignon, G. Wong, C. Earle, L. Chen, Hyaluronan-CD44v3 interaction with Oct4-Sox2-Nanog promotes miR-302 expression leading to self-renewal, clonal formation, and cisplatin resistance in cancer stem cells from head and neck squamous cell carcinoma, J. Biol. Chem. 287 (2012) 32800–32824.
[35] S. Volinia, G. Nuovo, A. Drusco, S. Costinean, R. Abujarour, C. Desponts, M. Garofalo, R. Baffa, R. Aeqilan, K. Maharry, M.E. Sana, G. Di Leva, P. Gasparini, P. Dama, J. Marchesini, M. Galasso, M. Manfrini, C. Zerbinati, F. Corra, T. Wise, S.E. Wojcik, M. Previati, F. Pichiorri, N. Zanesi, H. Alder, J. Palatini, K.F. Huebner, C.L. Shapiro, M. Negrini, A. Vecchione, A.L. Rosenberg, C.M. Croce, R. Garzon, Pluripotent stem cell miRNAs and metastasis in invasive breast cancer, J. Natl. Cancer Inst. 106 (2014).
[36] Y. Guo, J. Cui, Z. Ji, C. Cheng, K. Zhang, C. Zhang, M. Chu, Q. Zhao, Z. Yu, Y. Zhang, Y.X. Fang, W.Q. Gao, H.H. Zhu, miR-302/367/LATS2/YAP pathway is essential for prostate tumor-propagating cells and promotes the development of castration resistance, Oncogene 36 (2017) 6336–6347.
[37] E.L. Deer, J. Gonzalez-Hernandez, J.D. Coursen, J.E. Shea, J. Ngatia, C.L. Scaife, M.A. Firpo, S.J. Mulvihill, Phenotype and genotype of pancreatic cancer cell lines, Pancreas 39 (2010) 425–435.
[38] B. Zhou, J.W. Xu, Y.G. Cheng, J.Y. Gao, S.Y. Hu, L. Wang, H.X. Zhan, Early detection of pancreatic cancer: where are we now and where are we going?, International journal of cancer, J. Int. Cancer 141 (2017) 231–241.
[39] A. Barroso-delJesus, C. Romero-Lopez, G. Lucena-Aguilar, G.J. Melen, L. Sanchez, G. Ligero, A. Berzal-Herranz, P. Menendez, Embryonic stem cell-specific miR302-367 cluster: human gene structure and functional characterization of its core promoter, Mol. Cell Biol. 28 (2008) 6609–6619.
[40] L. Chen, L. Heikkinen, K. Emily Knott, Y. Liang, G. Wong, Evolutionary conservation and function of the human embryonic stem cell specific miR-302/367 cluster, Comparative biochemistry and physiology, Part D, Genomics & proteomics 16 (2015) 83–98.
[41] A.E. Frampton, L. Castellano, T. Colombo, E. Giovannetti, J. Krell, J. Jacob, L. Pellegrino, L. Roca-Alonso, N. Funel, T.M. Gall, A. De Giorgio, F.G. Pinho, V. Fulci, D.J. Britton, R. Ahmad, N.A. Habib, R.C. Coombes, V. Harding, T. Knosel, J. Stebbing, L.R. Jiao, MicroRNAs cooperatively inhibit a network of tumor suppressor genes to promote pancreatic tumor growth and progression, Gastroenterology 146 (2014) 268–277 e218.
[42] T. Barrett, S.E. Wilhite, P. Ledoux, C. Evangelista, I.F. Kim, M. Tomashevsky, K.A. Marshall, K.H. Phillippy, P.M. Sherman, M. Holko, A. Yefanov, H. Lee, N. Zhang, C.L. Robertson, N. Serova, S. Davis, A. Soboleva, NCBI GEO: archive for functional genomics data sets–update, Nucleic Acids Res. 41 (2013) D991–995.
[43] J. Huynh, N. Etemadi, F. Hollande, M. Ernst, M. Buchert, The JAK/STAT3 axis: a comprehensive drug target for solid malignancies, Semin. Canc. Biol. 45 (2017) 13–22.
[44] S. Savas, G. Skardasi, The SWI/SNF complex subunit genes: their functions, variations, and links to risk and survival outcomes in human cancers, Crit. Rev. Oncol.-Hematol. 123 (2018) 114–131.
[45] P. Gandellini, V. Doldi, N. Zaffaroni, microRNAs as players and signals in the metastatic cascade: implications for the development of novel anti-metastatic therapies, Semin. Canc. Biol. 44 (2017) 132–140.
[46] M. Liu, X. Zhang, An integrated analysis of mRNA-miRNA transcriptome data revealed hub regulatory networks in three genitourinary cancers, Biocell 41 (2017) 19–26.
[47] K. Chen, J.J. Ge, S.X. Yan, S.B. Ke, Microarray gene expression profiling for identifying different responses to radiotherapy and chemoradiotherapy in patients with cervical cancer, Eur. J. Gynaecol. Oncol. 38 (2017) 106–112.